MCAK activity at microtubule tips regulates spindle microtubule length to promote robust kinetochore attachment

Sarah B. Domnitz,[1] Michael Wagenbach,[1] Justin Decarreau,[1] and Linda Wordeman[1,2]

[1]Department of Physiology and Biophysics, University of Washington School of Medicine, Seattle, WA 98195
[2]Center for Cell Dynamics, Friday Harbor Laboratories, University of Washington, Friday Harbor, WA 98250

Mitotic centromere-associated kinesin (MCAK) is a microtubule-depolymerizing kinesin-13 member that can track with polymerizing microtubule tips (hereafter referred to as tip tracking) during both interphase and mitosis. MCAK tracks with microtubule tips by binding to end-binding proteins (EBs) through the microtubule tip localization signal SKIP, which lies N terminal to MCAK's neck and motor domain. The functional significance of MCAK's tip-tracking behavior during mitosis has never been explained. In this paper, we identify and define a mitotic function specific to the microtubule tip–associated population of MCAK: negative regulation of microtubule length within the assembling bipolar spindle. This function depends on MCAK's ability to bind EBs and track with polymerizing nonkinetochore microtubule tips. Although this activity antagonizes centrosome separation during bipolarization, it ultimately benefits the dividing cell by promoting robust kinetochore attachments to the spindle microtubules.

Introduction

Mitotic centromere-associated kinesin (MCAK/Kif2C) is a potent depolymerizer of microtubules in cells and in vitro. Surprisingly, however, this potent microtubule depolymerizer tracks with assembling microtubule tips (Honnappa et al., 2009), demonstrating that MCAK tracks with microtubule tips by binding to end-binding proteins (EBs) through the microtubule tip localization signal SKIP, which lies N terminal to MCAK's neck and motor domain. When this SKIP domain is mutated, both the EB interaction and tip tracking are abolished. MCAK-EB binding is necessary for MCAK's full depolymerization activity in cells as a result of increased targeting of MCAK to the microtubule tip even though MCAK's catalytic activity is not altered by binding to EBs (Honnappa et al., 2009; Montenegro Gouveia et al., 2010). The functional implications for the cell of MCAK's ability to tip track via EBs are presently untested.

It has been observed that adding successively higher levels of MCAK protein to *Xenopus laevis* extracts leads to shorter spindles during meiotic spindle assembly (Ohi et al., 2007), leading the authors to speculate that this effect can be attributed to MCAK's effect on dynamic microtubule plus ends. We devised the tools to mechanistically test this hypothesis in human mitotic cells. We used MCAK-specific siRNA to deplete endogenous MCAK in HeLa cells and performed live-cell time-lapse microscopy during recovery from monastrol. Treating cells with monastrol, a membrane-permeable inhibitor of the kinesin Eg5, prevents centrosomes from separating as cells enter mitosis, which leads to accumulation of monopolar cells (Kapoor et al., 2000). Inhibition can be reversed by monastrol washout such that cells recover and centrosomes separate to form bipolar spindles, making this assay useful for studying spindle assembly. We used a series of mutant versions of MCAK that target the depolymerizer to defined regions of the mitotic spindle to rescue the effect of MCAK loss on the assembling spindles.

We find that MCAK's tip-tracking activity is required to suppress centrosome separation during bipolar spindle assembly. Why this activity would be useful to the cell at the time when spindles are being assembled becomes clear when kinetochore attachment is monitored via MAD1 binding. Cells depleted of MCAK assemble spindles with excessively long

Correspondence to Linda Wordeman: worde@uw.edu

Abbreviations used in this paper: ACA, anticentromere antibody; MCAK, mitotic centromere-associated kinesin; wt, wild type.

The Rockefeller University Press $30.00
J. Cell Biol. Vol. 197 No. 2 231–237
www.jcb.org/cgi/doi/10.1083/jcb.201108147

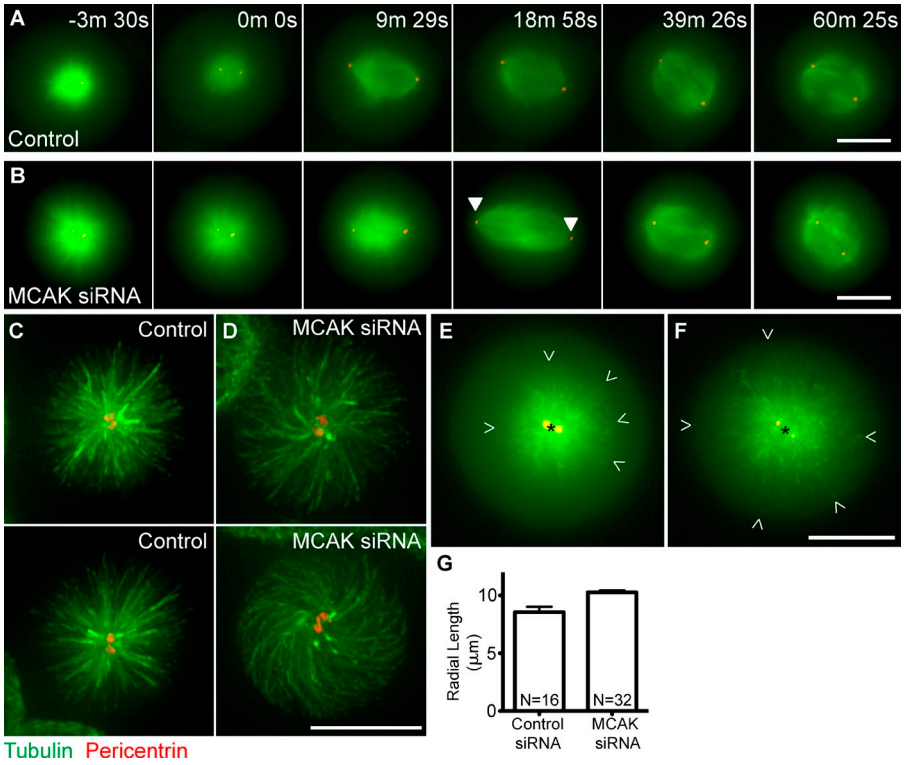

Figure 1. **MCAK depletion results in transient long spindles after monastrol washout.** (A) A cell treated with control siRNA. (B) A cell treated with MCAK-specific siRNA (arrowheads highlight centrosome position in long spindle). (C and D) Cells treated with control siRNA (C) or MCAK-specific siRNA (D) labeled with antitubulin and antipericentrin. Microtubule length can be measured in live cells expressing GFP-EB3 (green) and RFP-pericentrin (red). (E and F) The longest visible microtubule ends were measured in control (E) or MCAK siRNA-depleted (F) cells from the EB3-labeled tips (open arrowheads) to the center of the centrosomes (black asterisks). (G) Cell means of microtubule length in monasters in control siRNA and MCAK siRNA-depleted live cells. MCAK-depleted cells possess microtubules that are significantly longer ($P < 0.001$). Error bars correspond to SEM of cell means of the longest measurable microtubules. Bars, 10 µm.

nonkinetochore microtubules that elongate rapidly and to a greater extent than control cells. This activity can be rescued with wild-type (wt), but not a mutant, version of MCAK that is unable to track on assembling microtubule tips. The kinetochores in these spindles have difficulty establishing robust connections compared with control cells, as indicated by their high levels of MAD1. Thus, suppression of bipolarization by MCAK-dependent limits on microtubule length within the spindle has benefits for the cell in that it promotes robust attachment of kinetochores presumably by providing a high concentration of microtubule ends in the vicinity of congressing kinetochores.

Results and discussion

HeLa cells were transfected with constructs expressing RFP-pericentrin (to visualize centrosomes), EGFP-tubulin, and siRNA oligonucleotides directed against MCAK or nonspecific sequence (control) for 24 h and then incubated for 2 h in media containing 100 µM monastrol to accumulate monopolar spindles. At this time, unusually long microtubules were seen in monopolar cells depleted of endogenous MCAK (3-min, 30-s time point; Fig. 1 B). Monastrol-containing media was washed out, and cells were released into media containing 5 µM MG132 to prevent cells from progressing beyond metaphase. Control cells formed normal metaphase-length spindles of 10–12 µm after monastrol washout (Fig. 1 A and Video 1). In contrast, cells depleted of MCAK formed extremely long spindles (approaching 18 µm) 20 min after monastrol washout that appeared to be the product of long microtubules (18-min, 58-s time point; Fig. 1 B and Video 2). Microtubules appeared longer in MCAK-depleted monasters (Fig. 1, C and D) and in extreme cases exhibited curvature (Fig. 1 D, bottom). The cell means for the longest measurable microtubule lengths in live siRNA-treated cells dually expressing GFP-EB3 and RFP-pericentrin were significantly ($P < 0.001$) longer in MCAK-depleted cells (Fig. 1, E–G). The microtubule length measurements for MCAK-depleted cells may, in some cases, be an underestimate, as the microtubules may curve (Fig. 1 D, bottom). Interestingly, during monastrol reversal, the appearance of long spindles was transient, and, by 40 min after washout, spindle length had shortened, resulting in metaphase spindles similar in length to those of control cells. The transient nature of the spindle length overshoot is a likely explanation for why this effect has not been previously observed in standard MCAK depletions (Ganem et al., 2005; Wordeman et al., 2007). We conclude that MCAK suppresses spindle elongation by limiting microtubule length during bipolar spindle assembly in mammalian cells.

During interphase, MCAK localizes to polymerizing microtubule tips (Fig. 2 A; Moore et al., 2005). Mutating the SKIP domain in MCAK so that it cannot bind to the EBs (Fig. 2 B) impairs cellular microtubule depolymerization activity (Fig. 2 C; Montenegro Gouveia et al., 2010). During mitosis, MCAK localizes to centromeres, centrosomes, and polymerizing microtubule tips (Fig. 2 D; Wordeman and Mitchison, 1995). However, the mitotic role, if any, of the microtubule tip–associated population of MCAK remains unknown. As long microtubules correlated with the appearance of long spindles in cells depleted of MCAK (Fig. 1 B), we hypothesized that the mitotic role of MCAK concentrated at microtubule plus ends is to provide the depolymerization activity required to limit microtubule length and prevent long transient spindles during bipolar spindle assembly. Before directly testing this hypothesis, we compared GFP-wtMCAK with a version of MCAK in which the SKIP domain was mutated to SKNN (hereafter referred to as GFP-IPNN) in

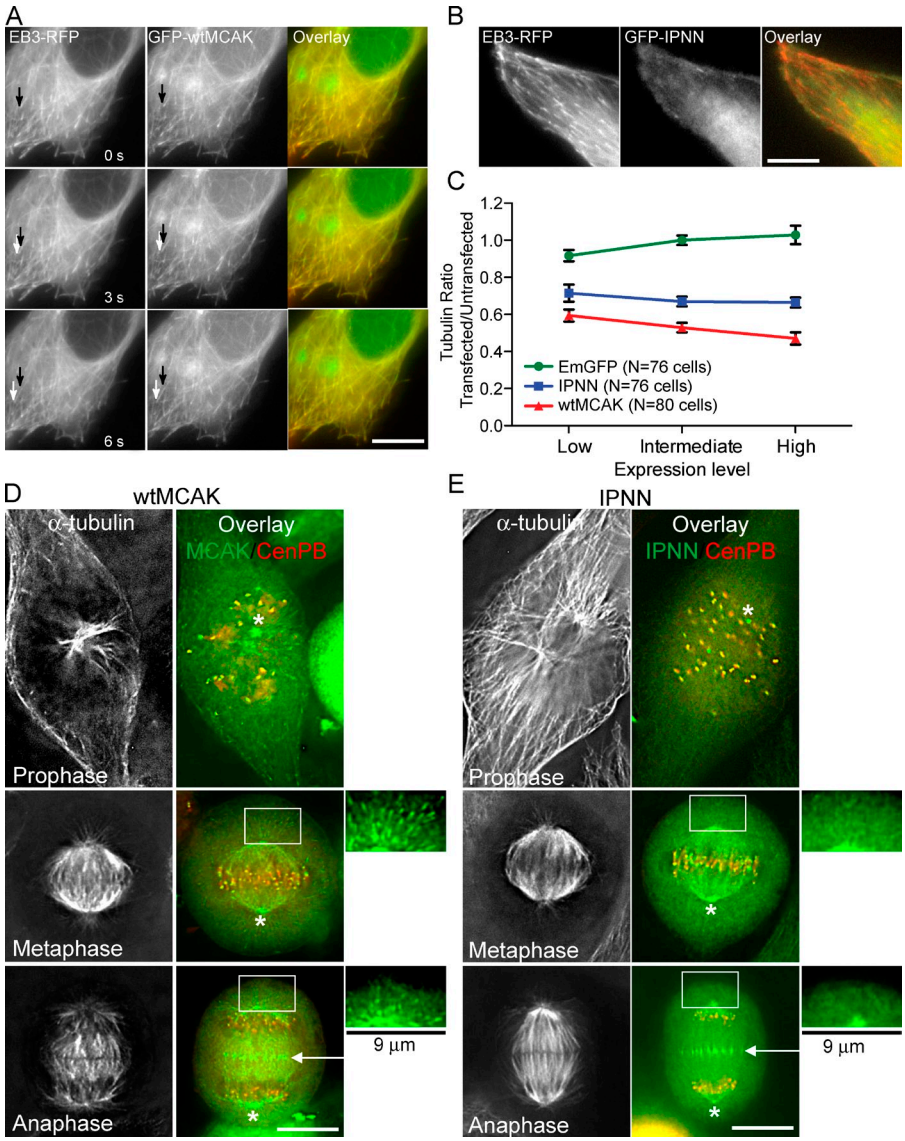

Figure 2. **EB binding is necessary for MCAK to concentrate on microtubule tips.** (A) Live imaging of a HeLa cell cotransfected with EB3-RFP and GFP-wtMCAK. Black arrows indicate the position of the polymerizing microtubule tip at a time of 0 s and later (white arrows). (B) A live cell cotransfected with EB3-RFP and GFP-IPNN-MCAK. (C) EB interaction correlates with less microtubule polymer in fixed interphase cells transfected with GFP-wtMCAK versus GFP-IPNN-MCAK or GFP. Error bars correspond to the SEM of the cell pair means of the tubulin ratios between a transfected and untransfected cell in the same field. (D) Fixed HeLa cells transfected with RFP–CENP-B (to mark centromeres; red) and EGFP-wtMCAK or EGFP-IPNN (green) and stained for α-tubulin. EGFP-wtMCAK concentrates at centrosomes (asterisks), centromeres, the spindle midzone (arrows), and microtubule tips (boxes and magnified images). (E) EGFP-IPNN localizes to centrosomes (asterisks), centromeres, and the spindle midzone (arrows) but not at microtubule tips (shown by the boxes and magnified images). Bars: (A, B, D, and E) 10 µm; (D and E, insets) 9 µm.

mitotic HeLa cells. This MCAK mutant cannot bind EBs or track with polymerizing microtubule tips (Fig. 2 B; Honnappa et al., 2009). We examined whether the binding interaction between MCAK and EBs is the principle determining factor for MCAK's concentration on microtubule tips during mitosis. Similar to GFP-wtMCAK, GFP-IPNN localized to centrosomes and centromeres throughout mitosis and to the spindle midzone during anaphase (Fig. 2, D and E). However, unlike GFP-wtMCAK, GFP-IPNN did not concentrate at polymerizing microtubule tips. This was most easily seen on the astral microtubules (magnified images in Fig. 2, D and E). We did not detect any significant difference in centromere activity between GFP-wtMCAK and GFP-IPNN (Fig. S1, A–E). To measure centrosome-specific differences between these two versions of MCAK, we depolymerized microtubules with nocodazole to reduce differences in MCAK concentration near the centrosome as a result of microtubule nucleation. We were unable to completely eliminate all microtubule polymers in the vicinity of the asters (unpublished data). The ratios were very similar, although GFP-IPNN was slightly higher (Fig. S1 F), possibly as a result of a separate contribution from GFP-wtMCAK tracking on the small amount of residual polymer.

To test our hypothesis that MCAK concentrated at polymerizing microtubule tips was responsible for the suppression of spindle elongation, cells depleted of endogenous MCAK were rescued with siRNA-resistant GFP-wtMCAK, GFP-IPNN, or GFP for 24 h. More than 80% depletion of endogenous MCAK can be achieved using this method (Fig. 3 A). Monastrol treatment and washout were performed in the same manner as for the live-cell microscopy assay (Fig. 1). Cells were fixed at −5, 20, 40, and 60 min after washout, and spindle length (based on distance between centrosomes) as a function of GFP expression was measured. Compared with cells expressing only GFP, spindle length was shorter in cells expressing an intermediate or high level of GFP-IPNN at each time point, although by 60 min after monastrol washout, spindles had reached the same length as those in cells expressing GFP (Fig. 3, B and C). The shorter spindle lengths in cells expressing GFP-IPNN compared with cells expressing GFP at 20 and 40 min are a result of GFP-IPNN that depolymerizes microtubules by reaching the microtubule tip

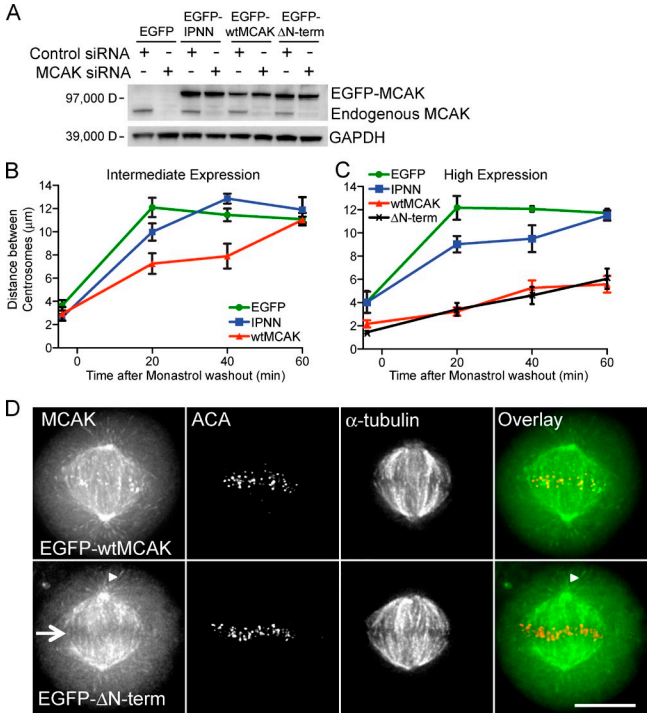

Figure 3. **MCAK suppresses centrosome separation and spindle length after monastrol washout by action at nonkinetochore microtubule tips.** (A) A Western blot demonstrating depletion of endogenous MCAK protein with MCAK-specific siRNA and rescue with EGFP constructs in HeLa cell lysates. HeLa cells depleted of endogenous MCAK and rescued with EGFP (control), EGFP-IPNN, EGFP-wtMCAK, or EGFP–ΔN-term are shown. GAPDH, glyceraldehyde 3-phosphate dehydrogenase. (B) Intermediate expression of EGFP-IPNN and EGFP-wtMCAK suppresses spindle length compared with EGFP, but centrosomes still separate to form normal-length bipolar spindles. (C) High expression of EGFP-wtMCAK or EGFP–ΔN-term inhibits centrosome separation, whereas cells expressing EGFP or EGFP-IPNN form bipolar spindles. (B and C) Error bars are SEM. The data were thresholded to three expression levels from cell means of centrosome distances at four time points. There were no less than 75 cells measured for each construct at each time point. The total numbers of cells measured are 343 (GFP), 360 (IPNN), 401 (wtMCAK), and 339 (ΔN-term). (D) Images of metaphase cells expressing EGFP-wtMCAK or EGFP–ΔN-term. Note that EGFP–ΔN-term is absent from centromeres (arrow) but is present on microtubule tips (arrowheads) and at the centrosome. ACA and tubulin staining are shown. Bar, 10 μm.

via 3D diffusion through the cytoplasm. Spindle length in cells expressing an intermediate level of GFP-wtMCAK was shorter than in cells expressing GFP or GFP-IPNN (Fig. 3 B), whereas cells expressing a high level of GFP-wtMCAK failed to establish a normal metaphase spindle length even 60 min after monastrol was washed out, demonstrating an MCAK-related, dose-dependent negative effect on spindle length (Figs. 3 C and S2). Collectively, these data indicate that MCAK's tip-tracking activity limits spindle length before metaphase. It is important to note that the mean spindle length in cells depleted of endogenous MCAK and rescued with GFP or GFP-IPNN does not approach 18 μm at the 20-min time point after monastrol washout, as might be expected based on live imaging of MCAK-depleted cells such as the cell shown in Fig. 1. Our fixed and live imaging data suggest that there is temporal variability in the time at which spindles reach their longest length. Therefore, when many cells are averaged together, the mean spindle length is shorter than the maximum length seen in live images. This is a likely explanation for

Table 1. **Distance between centrosomes is negatively correlated with increasing MCAK expression, as determined by Pearson correlation coefficients.**

	Time after MG132 added	Cells	Correlation coefficient	P-value
	min	*n*		
EGFP	−5	76	0.1399	0.228
	20	115	0.1728	0.065
	40	73	−0.0031	0.979
	60	79	−0.0516	0.651
IPNN	−5	88	0.0879	0.416
	20	123	−0.2288	0.011
	40	75	−0.3340	0.003
	60	74	−0.0019	0.987
wtMCAK	−5	95	−0.2078	0.043
	20	128	−0.6308	<0.0001
	40	104	−0.8081	<0.0001
	60	75	−0.7557	<0.0001

Pearson correlation coefficients for data are shown in Fig. 4, showing distance between centrosomes versus EGFP expression.

why the effect of MCAK on spindle lengths is controversial and inconsistent (Ganem et al., 2005; Buster et al., 2007; Wordeman et al., 2007).

There was a significant negative correlation between spindle length and extent of GFP-wtMCAK expression at all four time points, as determined by Pearson correlation coefficient, but there was no correlation between extent of GFP expression and spindle length at any time point (Table 1). This correlation is also supported by work in *Xenopus* extracts, which shows a negative correlation between bipolar spindle assembly and MCAK activity (Mitchison et al., 2005; Ohi et al., 2007; Cross and Powers, 2011). There was a small negative correlation at the 20- and 40-min time points in cells expressing GFP-IPNN, which was not unexpected, as GFP-IPNN can depolymerize microtubules if it contacts microtubule tips while diffusing in the cytoplasm. Higher expression of GFP-IPNN increases the amount of GFP-IPNN in the cytoplasm and therefore increases the amount of GFP-IPNN that comes in contact with microtubule tips. The negative correlation is stronger for GFP-wtMCAK, as higher expression increases GFP-wtMCAK at the polymerizing microtubule tips through tip tracking and through contact in the cytoplasm.

To confirm that the effect we saw on spindle length was a result of MCAK activity at microtubule tips rather than activity at centromeres, we engineered an MCAK mutant that was absent from centromeres (Maney et al., 2001; Walczak et al., 2002) but remained on microtubule tips and centrosomes by deleting the first 19 amino acids from the N terminus of MCAK (hereafter referred to as GFP–ΔN-term, Fig. 3 D). At each time point in our monastrol washout assay, spindle length in cells with high expression levels of GFP–ΔN-term was the same as it was in cells expressing high levels of GFP-wtMCAK (Fig. 3 C). These data define a role for the tip-tracking population of MCAK in regulating spindle length. In contrast, centromere-associated MCAK did not contribute to this process. Using monastrol, microtubules remain polymeric throughout the assay so that we were not studying microtubule nucleation. Thus, our results are not in

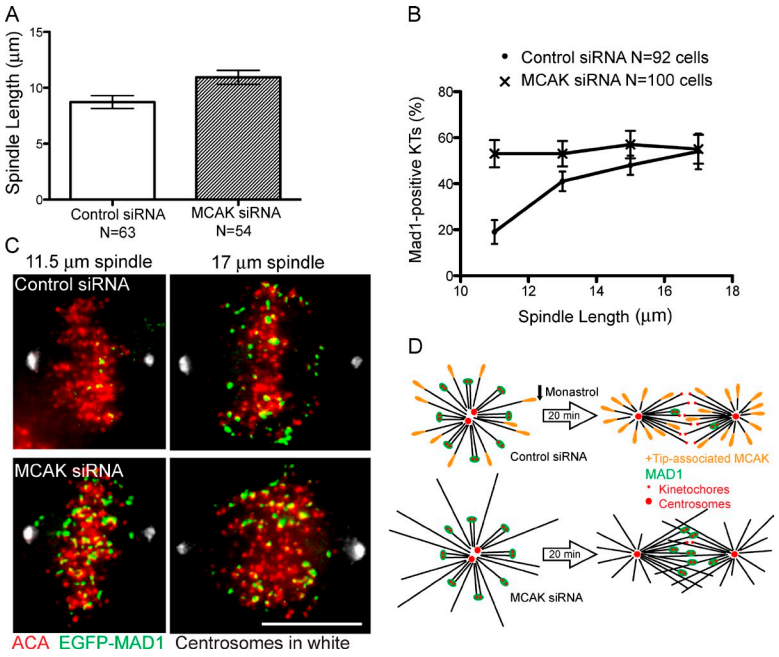

Figure 4. **Long microtubules correlate with a higher percentage of MAD1-positive kinetochores.** HeLa cells were transfected with EGFP-MAD1 and the indicated siRNA for 24 h before monastrol treatment. (A) Mean spindle length at 20 min after monastrol release for cells treated with MCAK-specific siRNA or control siRNA. N equals cell count. P = 0.01. (B) Percentage of Mad1-positive kinetochores (KTs) in cells treated as in A. (A and B) Error bars indicate SEM. (C) Spindles of different lengths showing kinetochores and the presence of MAD1 in cells treated as in A. Bar, 10 µm. (D) A model illustrating that in bipolar cells with long microtubules, free microtubule ends cross the metaphase plate and thus bypass many kinetochores so those kinetochores have more difficulty forming stable attachments to microtubules. As a result, MAD1 remains on these kinetochores.

conflict with previous work showing that centromeric MCAK inhibits microtubule nucleation and resulting spindle assembly (Tulu et al., 2003; Toso et al., 2009).

Depletion of MCAK from microtubule tips created very long spindles in our assay, but they were transient and eventually established normal-length metaphase spindles. This suggests that there are forces maintaining spindle length during metaphase in spite of the presence of long nonkinetochore microtubules and depleted endogenous MCAK levels. It is likely that numerous regulators of microtubule length may specifically control later stages of bipolar spindle assembly (Mitchison et al., 2005; McNally et al., 2006; Buster et al., 2007; Loughlin et al., 2011).

Previous studies have reported that MCAK depletion causes bipolar spindle collapse (Kollu et al., 2009; Tanenbaum et al., 2009), which would seem at odds with our finding that MCAK depletion transiently increases spindle length. However, these previous studies measured MCAK's effect on preestablished metaphase spindles in the absence of Eg5 activity, whereas we have measured MCAK's effect on bipolar spindles assembling in the presence of Eg5 activity. It is reasonable that exceptionally long microtubules, as caused by MCAK depletion, might lead to spindle collapse in the absence of Eg5 and excessive spindle elongation when Eg5 is present. Therefore, our results are not in conflict with past studies, but, rather, we define the contribution of MCAK activity as suppression of centrosome separation during bipolar spindle assembly.

Why is it important to regulate microtubule length during the establishment of spindle bipolarity? To determine the negative impact of long spindles composed of long microtubules, we used GFP-MAD1 as a sensitive readout for the stability of microtubule–kinetochore attachments. As microtubule-binding sites on kinetochores are filled, MAD1 disappears (Chen et al., 1998), making it a useful tool to study attachment defects. We evaluated cells transfected with GFP-MAD1 and either MCAK siRNA or control siRNA 20 min after monastrol washout. The mean spindle length was longer in MCAK-depleted cells than in control cells at 20 min after washout, consistent with transient excessive centrosome separation (Fig. 4 A). We measured GFP-MAD1–positive kinetochores in both control and MCAK-depleted cells with spindles that were 10 µm or longer to limit our study to established bipolar spindles. In control cells, we saw a positive correlation between spindle length and percentage of kinetochores that were positive for GFP-MAD1 20 min after washout (Fig. 4, B and C). In other words, control spindles that had achieved their normal metaphase length of 10–12 µm had less GFP-MAD1 on their kinetochores, suggestive of improved kinetochore–microtubule attachments, whereas control spindles that were unusually long exhibited poorly attached kinetochores. In MCAK-depleted cells, there were significantly more excessively long (>12 µm) spindles, and these spindles exhibited poor attachments (Fig. 4, B and C). What was surprising was that in contrast to control cells, MCAK-depleted cells had a high percentage of MAD1-positive kinetochores regardless of spindle length. Spindles that had achieved a normal metaphase length of 10–12 µm still exhibited very poorly attached kinetochores (Fig. 4, B and C). Live imaging of kinetochores establishing connections is shown in Video 3. We propose that MCAK-depleted cells have a high percentage of MAD1-positive kinetochores because MCAK depletion results in long microtubules at all spindle lengths during spindle assembly. Control cells likely have occasional long spindles as a result of long microtubules resulting from variability in endogenous levels of microtubule depolymerizers and stabilizers. Our results suggest that congressing kinetochores have trouble collecting sufficient numbers of end-on attachments to satisfy the spindle checkpoint when the spindle microtubules are long. Fig. 4 D illustrates this idea. Long microtubules lead to a lower concentration of free microtubule ends at the metaphase plate with which congressed kinetochores can form attachments.

Our data suggest that Eg5-dependent bipolar spindle length is amplified by long microtubules at early stages of centrosome separation. GFP-wtMCAK suppresses centrosome separation by efficiently depolymerizing microtubules and keeping them shorter in length. In contrast, in MCAK-depleted cells, the GFP-IPNN mutant has impaired depolymerization activity and fails to rescue extremely long spindles at levels in which GFP-wtMCAK succeeds in rescuing this effect. Thus, maintaining a shorter spindle length by restricting microtubule length is the responsibility of the population of MCAK molecules that are specifically recruited to polymerizing microtubule tips by EBs. In turn, this activity promotes proper kinetochore attachment by increasing the likelihood that kinetochores will encounter microtubule ends in the vicinity of the metaphase plate.

Centromere-associated MCAK utilizes its microtubule-depolymerizing activity (Hunter et al., 2003) to promote the turnover of microtubules at the kinetochore (Manning et al., 2007), which repairs aberrant microtubule connections and suppresses chromosome instability (Bakhoum et al., 2009). In contrast, MCAK that is recruited to microtubule ends via EB1 uses its microtubule-depolymerizing activity for a distinctly different cellular function: limiting microtubule length within the assembling spindle. Counter intuitively, this activity ensures proper kinetochore attachment and satisfaction of the spindle assembly checkpoint by increasing the density of microtubule ends in the spindle midzone. The importance of this activity for achieving robust microtubule attachment cannot be overemphasized. Kinetochores can use either CENP-E–directed gliding to a microtubule plus end (Kapoor et al., 2006; Kim et al., 2008; Cai et al., 2009; Magidson et al., 2011) or dynein-dependent minus-end–directed gliding to the centrosome (Yang et al., 2007) to position themselves in juxtaposition to high concentrations of microtubule ends. However, excessively long microtubules will dilute the concentration of ends in the spindle midzone as some microtubules will extend toward the opposite half spindle. We hypothesize that this defeats the purpose of lateral gliding to achieve amphitelic attachments because, once bound to the end of the microtubule, the options for further microtubule capture by the kinetochore are constrained because their mobility is limited by the dynamics of the attached microtubules. This, we hypothesize, may be the purpose of congression in organisms possessing kinetochores that bind multiple microtubules. If microtubule length within the bipolar spindle is not constrained, then the proportion of microtubule plus ends in the vicinity of the kinetochores will be insufficient, leading to difficulty in satisfying the checkpoint and increased chromosome instability.

Materials and methods

Cell culture, transfection, and immunofluorescence

HeLa cells were grown in MEM Alpha medium (Invitrogen) supplemented with 10% FBS (Hyclone; Thermo Fisher Scientific). Cells were transfected with 2 µg of plasmid DNA by electroporation with Nucleofector II (Lonza) according to manufacturer's instructions. Cells were also transfected with 33 nM MCAK siRNA using the transfection reagent Lipofectamine RNAiMAX (Invitrogen). Cells were seeded on 12-mm coverglasses and incubated for 24 h at 37°C in 5% CO_2. Cells were treated with media containing 100 µM monastrol (A.G. Scientific, Inc.) for 2 h. Monastrol was quickly washed out three times with fresh media and then replaced with media containing 5 µM MG132 (EMD) for 20–60 min. Cells were fixed in 1% PFA in −20°C methanol for 10 min or 0.5% glutaraldehyde in PBS at 37°C for 10 min followed by 0.2% Triton X-100 in PBS for 10 min and then quenched in 0.1% sodium borohydride three times for 10 min. Cells were stained with anti–γ-tubulin primary antibody (Sigma-Aldrich) followed by Texas red donkey anti–mouse secondary antibody (Jackson ImmunoResearch Laboratories, Inc.) or anti–human anticentromere antibody (ACA) primary antibody (Antibodies Inc.) followed by Alexa Fluor 568 goat anti–human secondary antibody (Invitrogen). All cells were stained with YL (rat antityrosinated tubulin ab6160; Abcam) anti–α-tubulin primary antibody followed by Cy5 anti–rat secondary antibody (Jackson ImmunoResearch Laboratories, Inc.). Coverglasses were mounted with DAPI-containing VECTASHIELD mounting medium (Vector Laboratories).

siRNA and DNA constructs

Endogenous MCAK was depleted with siRNA (ID no. s21665; Applied Biosystems). Where indicated, mock siRNA was used as a control (negative control no. 1; Applied Biosystems). An siRNA-resistant CgMCAK plasmid, EGFP-wtMCAK, was derived from full-length MCAK (Ovechkina et al., 2002) by oligonucleotide-directed mutagenesis (Sambrook et al., 1989) to alter MCAK codons 60–64 of 5′-GCAATAAACCCAGAA-3′ by silent substitutions of sequence 5′-GCcATcAAtCCgGAg-3′, in which lowercase letters indicate mismatches with siRNA no. s21665. Mutations I97N and P98N were introduced by PCR into EGFP-wtMCAK to give EGFP-IPNN. A deletion of the first 19 codons was introduced by PCR into EGFP-wtMCAK to give EGFP–ΔN-term.

SDS-PAGE and Western blotting

HeLa cells were lysed, and proteins were separated and visualized as previously described (Rankin and Wordeman, 2010), with the exception that cells were lysed 24 h after transfection.

Fixed-cell microscopy

Cells were imaged on a widefield microscope (model FX-A; Nikon) with a cooled charge-coupled device camera (SenSys; Photometrics) controlled by QED camera software (Media Cybernetics). For each time point during the monastrol washout assay, all cells between the monopole phase and metaphase were counted, provided both centrosomes were in the same plane of focus. Multipolar cells, which were in the minority, were excluded, regardless of cell cycle phase and even if all poles were in the same plane of focus.

Quantification of fixed-cell images

Distance between γ-tubulin–labeled centrosomes was measured in ImageJ (National Institutes of Health). Mean EGFP expression for each cell was determined by encircling the cell and obtaining the mean pixel intensity. Sister centromere separation was calculated by measuring the centroid-to-centroid distance between RFP–CENP-B–labeled centromeres in ImageJ. Statistical significance for datasets was determined by a two-tailed unpaired Student's *t* test in Excel (Microsoft). Pearson correlation coefficients were determined using Prism (version 5.0c; GraphPad Software). The percentage of MAD1-positive kinetochores was calculated by counting the number of MAD1-labeled kinetochores per cell divided by the number of ACA-stained kinetochores per cell. Only cells with a spindle length of 10 µm or more were measured.

Quantification of turnover at the centromere

HeLa cells were transfected with either EmGFP-wtMCAK or EmGFP-IPNN. Individual centromeres in live transfected cells were bleached with one 200-ms pulse at 17% laser power from a 406-nm laser using a FRAP-enabled DeltaVision RT system (Applied Precision) and a 1.4 NA 100× objective (Olympus). Postbleach images were collected adaptively using a 32% neutral density filter and ranging from 2-ms to 3-s intervals. Under these conditions, no bleach decay was observed after recovery. The fluorescence of the bleached centromere region was measured in arbitrary units, and the time and extent of recovery were plotted using a single-phase exponential in Prism (version 5.0).

Live-cell imaging

HeLa cells were cultured and transfected as described for fixed-cell assay but plated on 35-mm glass coverslip dishes coated with poly-L-lysine (MatTek Corporation) for 24 h after DNA and siRNA transfections but before live imaging analysis. Before imaging, cells were switched to 37°C CO_2-independent media (Invitrogen) with 10% FBS. Monastrol was washed out, and cells were released into 5 µM MG132. Time is reported relative to addition of MG132. Cells were imaged with a DeltaVision RT system equipped

with an inverted microscope (IX-71; Olympus) and softWoRx (version 3.6.0; Applied Precision) with 3D rendering. A CoolSNAP HQ2 camera (Photometrics) with an intensity offset set to 50.00 was used to record the images. Images were collected with a 60× 1.42 NA objective (Olympus) and a 37°C environmental chamber (Applied Precision). Images were collected by a 10.2-µm optical axis integration scan (Applied Precision) at 30-s intervals. Subsequent deconvolution was performed with bleach correction and z line correction "on" in the softWoRx menu. Monastrol washout was performed during imaging, as described for fixed cells.

Online supplemental material

Fig. S1 shows that loss of tip-tracking activity does not alter MCAK's activity at the centrosome or centromere. Fig. S2 presents histograms of the data supporting the discovery that EGFP-wtMCAK suppresses spindle length during assembly compared with EGFP-IPNN and EGFP control. Video 1 records a HeLa cell transfected with control siRNA and constructs expressing RFP-pericentrin and GFP-tubulin recovering from monastrol treatment. Video 2 shows a similar cell recovering from monastrol treatment, except that it has been transfected with siRNA directed against endogenous MCAK; the assembling spindle exhibits a length overshoot during bipolarization. Video 3 shows a control and MCAK siRNA-treated cell expressing GFP-Mad1 and recovering from monastrol treatment, illustrating the preferential retention of GFP-MAD1 on MCAK-depleted spindles. Online supplemental material is available at http://www.jcb.org/cgi/content/full/jcb.201108147/DC1.

We are grateful to Jason Stumpff and Andy Powers for comments on the manuscript.

This work was supported by National Institutes of Health grants to L. Wordeman (GM69429) and S.B. Domnitz (GM007270) and by the University of Washington Molecular Medicine program.

Submitted: 24 August 2011
Accepted: 7 March 2012

References

Bakhoum, S.F., S.L. Thompson, A.L. Manning, and D.A. Compton. 2009. Genome stability is ensured by temporal control of kinetochore-microtubule dynamics. *Nat. Cell Biol.* 11:27–35. http://dx.doi.org/10.1038/ncb1809

Buster, D.W., D. Zhang, and D.J. Sharp. 2007. Poleward tubulin flux in spindles: Regulation and function in mitotic cells. *Mol. Biol. Cell*. 18:3094–3104. http://dx.doi.org/10.1091/mbc.E06-11-0994

Cai, S., C.B. O'Connell, A. Khodjakov, and C.E. Walczak. 2009. Chromosome congression in the absence of kinetochore fibres. *Nat. Cell Biol.* 11:832–838. http://dx.doi.org/10.1038/ncb1890

Chen, R.H., A. Shevchenko, M. Mann, and A.W. Murray. 1998. Spindle checkpoint protein Xmad1 recruits Xmad2 to unattached kinetochores. *J. Cell Biol.* 143:283–295. http://dx.doi.org/10.1083/jcb.143.2.283

Cross, M.K., and M.A. Powers. 2011. Nup98 regulates bipolar spindle assembly through association with microtubules and opposition of MCAK. *Mol. Biol. Cell*. 22:661–672. http://dx.doi.org/10.1091/mbc.E10-06-0478

Ganem, N.J., K. Upton, and D.A. Compton. 2005. Efficient mitosis in human cells lacking poleward microtubule flux. *Curr. Biol.* 15:1827–1832. http://dx.doi.org/10.1016/j.cub.2005.08.065

Honnappa, S., S.M. Gouveia, A. Weisbrich, F.F. Damberger, N.S. Bhavesh, H. Jawhari, I. Grigoriev, F.J. van Rijssel, R.M. Buey, A. Lawera, et al. 2009. An EB1-binding motif acts as a microtubule tip localization signal. *Cell*. 138:366–376. http://dx.doi.org/10.1016/j.cell.2009.04.065

Hunter, A.W., M. Caplow, D.L. Coy, W.O. Hancock, S. Diez, L. Wordeman, and J. Howard. 2003. The kinesin-related protein MCAK is a microtubule depolymerase that forms an ATP-hydrolyzing complex at microtubule ends. *Mol. Cell*. 11:445–457. http://dx.doi.org/10.1016/S1097-2765(03)00049-2

Kapoor, T.M., T.U. Mayer, M.L. Coughlin, and T.J. Mitchison. 2000. Probing spindle assembly mechanisms with monastrol, a small molecule inhibitor of the mitotic kinesin, Eg5. *J. Cell Biol.* 150:975–988. http://dx.doi.org/10.1083/jcb.150.5.975

Kapoor, T.M., M.A. Lampson, P. Hergert, L. Cameron, D. Cimini, E.D. Salmon, B.F. McEwen, and A. Khodjakov. 2006. Chromosomes can congress to the metaphase plate before biorientation. *Science*. 311:388–391. http://dx.doi.org/10.1126/science.1122142

Kim, Y., J.E. Heuser, C.M. Waterman, and D.W. Cleveland. 2008. CENP-E combines a slow, processive motor and a flexible coiled coil to produce an essential motile kinetochore tether. *J. Cell Biol.* 181:411–419. http://dx.doi.org/10.1083/jcb.200802189

Kollu, S., S.F. Bakhoum, and D.A. Compton. 2009. Interplay of microtubule dynamics and sliding during bipolar spindle formation in mammalian cells. *Curr. Biol.* 19:2108–2113. http://dx.doi.org/10.1016/j.cub.2009.10.056

Loughlin, R., J.D. Wilbur, F.J. McNally, F.J. Nédélec, and R. Heald. 2011. Katanin contributes to interspecies spindle length scaling in *Xenopus*. *Cell*. 147:1397–1407. http://dx.doi.org/10.1016/j.cell.2011.11.014

Magidson, V., C.B. O'Connell, J. Lončarek, R. Paul, A. Mogilner, and A. Khodjakov. 2011. The spatial arrangement of chromosomes during prometaphase facilitates spindle assembly. *Cell*. 146:555–567. http://dx.doi.org/10.1016/j.cell.2011.07.012

Maney, T., M. Wagenbach, and L. Wordeman. 2001. Molecular dissection of the microtubule depolymerizing activity of mitotic centromere-associated kinesin. *J. Biol. Chem.* 276:34753–34758. http://dx.doi.org/10.1074/jbc.M106626200

Manning, A.L., N.J. Ganem, S.F. Bakhoum, M. Wagenbach, L. Wordeman, and D.A. Compton. 2007. The kinesin-13 proteins Kif2a, Kif2b, and Kif2c/MCAK have distinct roles during mitosis in human cells. *Mol. Biol. Cell*. 18:2970–2979. http://dx.doi.org/10.1091/mbc.E07-02-0110

McNally, K., A. Audhya, K. Oegema, and F.J. McNally. 2006. Katanin controls mitotic and meiotic spindle length. *J. Cell Biol.* 175:881–891. http://dx.doi.org/10.1083/jcb.200608117

Mitchison, T.J., P. Maddox, J. Gaetz, A. Groen, M. Shirasu, A. Desai, E.D. Salmon, and T.M. Kapoor. 2005. Roles of polymerization dynamics, opposed motors, and a tensile element in governing the length of *Xenopus* extract meiotic spindles. *Mol. Biol. Cell*. 16:3064–3076. http://dx.doi.org/10.1091/mbc.E05-02-0174

Montenegro Gouveia, S., K. Leslie, L.C. Kapitein, R.M. Buey, I. Grigoriev, M. Wagenbach, I. Smal, E. Meijering, C.C. Hoogenraad, L. Wordeman, et al. 2010. In vitro reconstitution of the functional interplay between MCAK and EB3 at microtubule plus ends. *Curr. Biol.* 20:1717–1722. http://dx.doi.org/10.1016/j.cub.2010.08.020

Moore, A.T., K.E. Rankin, G. von Dassow, L. Peris, M. Wagenbach, Y. Ovechkina, A. Andrieux, D. Job, and L. Wordeman. 2005. MCAK associates with the tips of polymerizing microtubules. *J. Cell Biol.* 169:391–397. http://dx.doi.org/10.1083/jcb.200411089

Ohi, R., K. Burbank, Q. Liu, and T.J. Mitchison. 2007. Nonredundant functions of Kinesin-13s during meiotic spindle assembly. *Curr. Biol.* 17:953–959. http://dx.doi.org/10.1016/j.cub.2007.04.057

Ovechkina, Y., M. Wagenbach, and L. Wordeman. 2002. K-loop insertion restores microtubule depolymerizing activity of a "neckless" MCAK mutant. *J. Cell Biol.* 159:557–562. http://dx.doi.org/10.1083/jcb.200205089

Rankin, K.E., and L. Wordeman. 2010. Long astral microtubules uncouple mitotic spindles from the cytokinetic furrow. *J. Cell Biol.* 190:35–43. http://dx.doi.org/10.1083/jcb.201004017

Sambrook, J., E.F. Fritsch, and T. Maniatis. 1989. Molecular Cloning: A Laboratory Manual. Vol. 3. Cold Spring Harbor Laboratory, Cold Spring Harbor, NY. 1659 pp.

Tanenbaum, M.E., L. Macůrek, A. Janssen, E.F. Geers, M. Alvarez-Fernández, and R.H. Medema. 2009. Kif15 cooperates with eg5 to promote bipolar spindle assembly. *Curr. Biol.* 19:1703–1711. http://dx.doi.org/10.1016/j.cub.2009.08.027

Toso, A., J.R. Winter, A.J. Garrod, A.C. Amaro, P. Meraldi, and A.D. McAinsh. 2009. Kinetochore-generated pushing forces separate centrosomes during bipolar spindle assembly. *J. Cell Biol.* 184:365–372. http://dx.doi.org/10.1083/jcb.200809055

Tulu, U.S., N.M. Rusan, and P. Wadsworth. 2003. Peripheral, non-centrosome-associated microtubules contribute to spindle formation in centrosome-containing cells. *Curr. Biol.* 13:1894–1899. http://dx.doi.org/10.1016/j.cub.2003.10.002

Walczak, C.E., E.C. Gan, A. Desai, T.J. Mitchison, and S.L. Kline-Smith. 2002. The microtubule-destabilizing kinesin XKCM1 is required for chromosome positioning during spindle assembly. *Curr. Biol.* 12:1885–1889. http://dx.doi.org/10.1016/S0960-9822(02)01227-7

Wordeman, L., and T.J. Mitchison. 1995. Identification and partial characterization of mitotic centromere-associated kinesin, a kinesin-related protein that associates with centromeres during mitosis. *J. Cell Biol.* 128:95–104. http://dx.doi.org/10.1083/jcb.128.1.95

Wordeman, L., M. Wagenbach, and G. von Dassow. 2007. MCAK facilitates chromosome movement by promoting kinetochore microtubule turnover. *J. Cell Biol.* 179:869–879. http://dx.doi.org/10.1083/jcb.200707120

Yang, Z., U.S. Tulu, P. Wadsworth, and C.L. Rieder. 2007. Kinetochore dynein is required for chromosome motion and congression independent of the spindle checkpoint. *Curr. Biol.* 17:973–980. http://dx.doi.org/10.1016/j.cub.2007.04.056